Turkish J. Eng. Env. Sci.
34 (2010) , 1 – 15.

doi:10.3906/muh-1003-96

The effect of the initial stretching of the rectangular plate with a cylindrical hole on the stress and displacement distributions around the hole

Ülkü BABUŞÇU YEŞİL
Yıldız Technical University, Faculty of Chemical and Metallurgical Engineering,
Department of Mathematical Engineering, Davutpaşa Campus, 34210, Esenler, İstanbul-TURKEY
e-mail: ubabuscu@yildiz.edu.tr

Received 19.03.2010

Abstract

The effect of an initial stretching of a rectangular plate with a cylindrical hole on the stress and displacement distributions around the hole, which are caused by the additional loading, was studied using the finite element method. It is assumed that the initial stresses are caused by the uniformly stretching forces acting on the 2 opposite ends. It is also assumed that the cylindrical hole contained by the thick plate is between these ends and goes in parallel with them. The aim of the author is to analyze the effect of anisotropy and initial loading on the stress and displacement distributions around the cylindrical hole of the considered plate. The mathematical formulation of the corresponding boundary-value problem is presented within the framework of the 3-dimensional linearized theory of elasticity. In order to find a solution to this problem, the 3D finite element method was employed. The numerical results on the distribution of the stress and displacement distributions around the cylindrical hole and the influence of the initial forces, geometrical and mechanical parameters on these distributions are presented and discussed.

Key Words: Initial stretching force, stress concentration, cylindrical hole, composite thick plate, FEM (Finite Element Method)

Introduction

Holes in structural components can create stress concentration and hence reduce the mechanical properties. In other words, stress concentrations significantly affect the life of an engineering structure. Knowledge of stress concentration in the vicinity of a hole should be required for a reliable design of structural components. Particularly, the increasing use of composite materials in the structural elements requires a better understanding and modeling of the behavior of these structures.

There are many studies on the effects of holes on the static and dynamic characteristics of construction elements (Chaudhuri, 2007; Jain and Mittal, 2008; Lei et al., 2001; Savin, 1961; Temiz et al., 2003; Toubal et al., 2005; Zheng et al., 2008). Based on the analyses of the above-mentioned investigations, there are a few studies on the influence of the initial stresses arising as a result of initial stretching on the stress concentration

caused by an additional loading in the case where the superposition principle is not applicable (Akbarov et al., 2004; Akbarov et al., 2008; Yahnioglu and Babuscu Yesil, 2009). Here under non-applicability of the superposition principle it is understood that the stress field caused by the additional loading significantly depends on the initial loading. However, according to the well-known mechanical considerations for the cases where the magnitude of the initial loading is greater than that of the additional loading, these investigations can be carried out within the framework of the 3-dimensional linearized theory of deformable body (Guz, 1999).

The present study concerns stress and displacement distributions on an initially statically stressed thick rectangular composite plate which contains an internal cylindrical hole (lying width-wise in the plate) given a rectangular cross section with rounded off corners. The governing equation is derived within the scope of the 3-dimensional linearized theory of elasticity (TDLTE). Due to theoretical difficulties in dealing with complicated problems, the finite element method (FEM) is employed in order to solve the corresponding boundary-value problems in the determination of the initial stress-state, as well as in the determination of the stress-state for the additional static loading. The numerical results for the stress and displacement distributions around the hole are presented and the influence of the initial stresses and other problem parameters on these distributions are analyzed and discussed.

Formulation of the Problem

Consider a thick rectangular plate containing a cylindrical hole. Its geometry is shown in Figure 1. The Cartesian coordinate system $Ox_1x_2x_3$ is associated with the plate so as to give Lagrange coordinates in the initial state. Assume that the plate occupies the region $(\Omega - \Omega')$, where

$$\Omega = \{0 \le x_1 \le \ell_1;\ 0 \le x_2 \le h;\ 0 \le x_3 \le \ell_3\},$$

$$\Omega' = \left\{ \left(\frac{\ell_1}{2} - b + R\right) \le x_1 \le \left(\frac{\ell_1}{2} + b - R\right); h_A \le x_2 \le h - h_U;\ 0 \le x_3 \le \ell_3 \right\} \cup$$

$$\left\{ \begin{array}{l} (x_1, x_2, x_3) |\ (x_1 - x_{01})^2 + (x_2 - y_{01})^2 \le R^2, \\ \left(\frac{\ell_1}{2} - b\right) \le x_1 \le \left(\frac{\ell_1}{2} - b + R\right); h_A \le x_2 \le h - h_U;\ 0 \le x_3 \le \ell_3 \end{array} \right\} \cup$$

$$\left\{ \begin{array}{l} (x_1, x_2, x_3) |\ (x_1 - x_{02})^2 + (x_2 - y_{02})^2 \le R^2, \\ \left(\frac{\ell_1}{2} + b - R\right) \le x_1 \le \left(\frac{\ell_1}{2} + b\right); h_A \le x_2 \le h - h_U;\ 0 \le x_3 \le \ell_3 \end{array} \right\}. \quad (1)$$

In Eq. (1) (x_{01}, y_{01}) $((x_{02}, y_{02}))$ is the center of the left (right) half circular arc in the plane x_3= const. and h_A(h_U) is the height of the part of the plate at the bottom (top) of the hole. Suppose that the material of the strip is transversally isotropic with isotropy axis Ox_2. Moreover, assume that the plate is simply supported at all edge surfaces and in the initial state the uniformly distributed normal stretching forces with intensity q act on the surfaces $x_1 = 0$ and $x_1 = \ell_1$. The additional uniformly distributed normal forces with intensity p $(< q)$ act on the upper face plane of the plate. Hence, this problem is investigated in 2 parts: in the first part (initial state), the initial stress-state is determined for the uniformly distributed normal static forces q, and in the second part (perturbed state), the stress field under the action of the additional static forces on the upper face-plane of the initial stretching plate is determined. Through the investigation, all quantities referring to the initial state will be labeled by the superscript (0) and repeated indices are summed over their ranges.

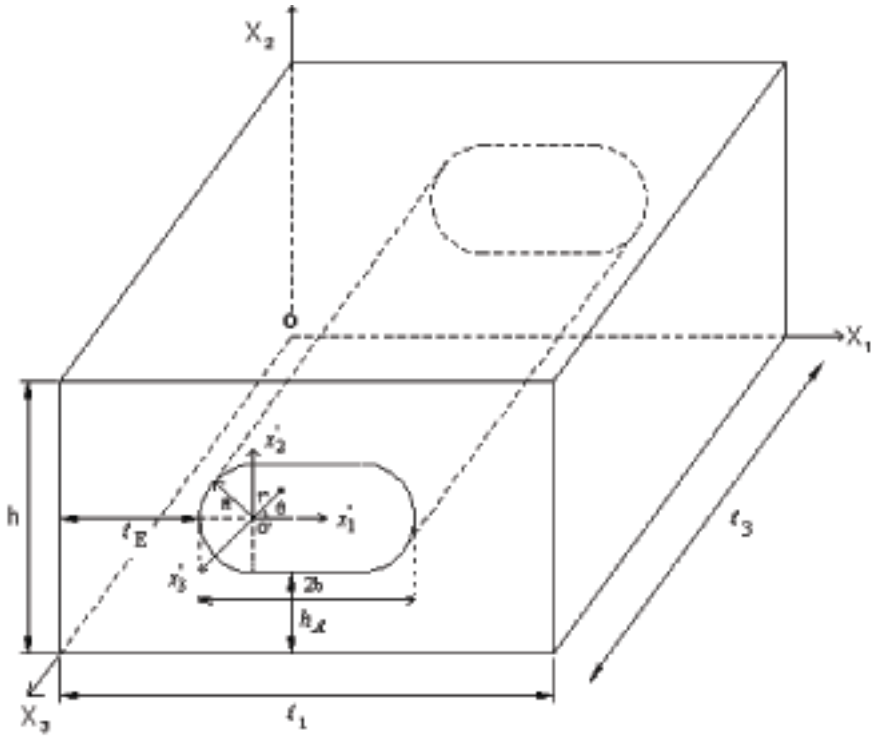

Figure 1. Considered plate geometry and some values of geometrical parameters.

According to the discussions above, the initial stress-state can be determined by the solution to the boundary-value problem given below.

$$\frac{\partial \sigma_{ij}^{(0)}}{\partial xj}=0; \quad \sigma^{(0)}=\mathbf{D}\varepsilon^{(0)}; \quad \sigma^{(0)}=\left\{\sigma_{ij}^{(0)}\right\}; \quad \varepsilon^{(0)}=\left\{\varepsilon_{ij}^{(0)}\right\}; \quad \varepsilon_{ij}^{(0)}=\frac{1}{2}\left(\frac{\partial u_i^{(0)}}{\partial x_j}+\frac{\partial u_j^{(0)}}{\partial x_i}\right)$$

$$\mathbf{D}=\begin{bmatrix} A_{11} & A_{12} & A_{13} & 0 & 0 & 0 \\ A_{12} & A_{22} & A_{23} & 0 & 0 & 0 \\ A_{13} & A_{23} & A_{33} & 0 & 0 & 0 \\ 0 & 0 & 0 & 2A_{44} & 0 & 0 \\ 0 & 0 & 0 & 0 & 2A_{55} & 0 \\ 0 & 0 & 0 & 0 & 0 & 2A_{66} \end{bmatrix}$$

$$u_{\ 2}^{(0)}\Big|_{x_1=0;\ell_1}=u_{\ 2}^{(0)}\Big|_{x_3=0;\ell_3}=0,\ \sigma_{1i}^{(0)}\Big|_{x_1=0;\ell_1}=q\delta_1^i,$$

$$\sigma_{2i}^{(0)}\Big|_{x_2=0;h}=0, \quad \sigma_{3i}^{(0)}\Big|_{x_3=0;\ell_3}=0, \quad \sigma_{ij}^{(0)}n_j\Big|_S=0, i;j=1,2,3. \tag{2}$$

In Eq. (2), A_{ij} are the material constants, δ_i^j is the Kronecker symbol, S shows the surface of the cylindrical hole, and n_j is the components of the unit normal vector to the surface S, and the other notation is conventional.

To determine the stress-state caused by the additional loading (i.e. the perturbed state), the following boundary-value problem must be solved:

$$\frac{\partial}{\partial x_j}\left(\sigma_{ji}+\sigma_{in}^{(0)}\frac{\partial u_i}{\partial x_n}\right)=0, \tag{3}$$

$$\sigma = \mathbf{D}\varepsilon; \quad \sigma^{(0)} = \left\{\sigma_{ij}^{(0)}\right\}; \quad \varepsilon^{(0)} = \left\{\varepsilon_{ij}^{(0)}\right\}; \quad \varepsilon_{ij} = \frac{1}{2}\left(\frac{\partial u_i}{\partial x_j} + \frac{\partial u_j}{\partial x_i}\right) \tag{4}$$

$$u_{\ 2}|_{x_1=0;\ell_1} = u_{\ 2}|_{x_3=0;\ell_3} = 0,$$

$$\left(\sigma_{1i} + \sigma_{in}^{(0)}\frac{\partial u_i}{\partial x_n}\right) n_1\Big|_{x_1=0;\ell_1} = 0,$$

$$\left(\sigma_{ji} + \sigma_{in}^{(0)}\frac{\partial u_i}{\partial x_n}\right) n_j\Big|_{x_2=h} = p\delta_2^i, \quad \left(\sigma_{ji} + \sigma_{in}^{(0)}\frac{\partial u_i}{\partial x_n}\right) n_j\Big|_{x_2=0} = 0,$$

$$\left(\sigma_{3i} + \sigma_{1n}^{(0)}\frac{\partial u_i}{\partial x_n}\right) n_3\Big|_{x_3=0;\ell_3} = 0,$$

$$\left(\sigma_{ji} + \sigma_{in}^{(0)}\frac{\partial u_i}{\partial x_n}\right) n_j\Big|_{S} = 0, i; j = 1, 2, 3. \tag{5}$$

Note that the equations and relations given in Eqs. (3-5) are the corresponding ones for TDLTE as written in References. (Akbarov et al., 2004; Akbarov et al., (2008); Guz, 1999). Thus, the mathematical formulation of the problem considered has been exhausted. Note that the solution to the boundary-value problem (2) gives us the distributions of the initial stresses and the solution to the boundary-value problems (3-5) gives us the distributions of the stresses and displacements under the additional forces acting on the upper face plane of the plate. Moreover, the field equations of the second boundary-value problem contain the functions determined by the solution to the first boundary-value problem. Therefore, the second boundary-value problem can be solved after the first boundary-value problem.

1. FEM Modeling

For the FEM modeling of the boundary-value problem in Eq. (2), the functional

$$\Pi^{(0)} = \frac{1}{2}\iiint\limits_{\Omega-\Omega'} \sigma_{ij}^{(0)}\varepsilon_{ij}^{(0)}d\Omega - \iint\limits_{S_q} \sigma_{ij}^{(0)}n_j u_i^{(0)}dS_q \tag{6}$$

is used. However, for the FEM modeling of (3-5) according to [11], the functional

$$\Pi = \frac{1}{2}\iiint\limits_{\Omega-\Omega'} T_{ij}\frac{\partial u_j}{\partial x_i}d\Omega - \iint\limits_{S_p} T_{ij}n_j u_i dS_p \tag{7}$$

is employed, where

$$T_{ij} = \sigma_{ij} + \sigma_{ij}^{(0)}\frac{\partial u_i}{\partial x_n}. \tag{8}$$

In Eq. (8) the stresses $\sigma_{ij}^{(0)}$ are called the initial stresses and determined from the solution of the boundary-value problem given in Eq. (2). For each functional, using the virtual work principle and employing the well known Ritz technique, FEM modeling of each problem is obtained. In this case, the solution domain is divided into a finite number of triangular prism elements with 6 nodes (for the surrounding of the cylindrical hole) and brick elements with 8 nodes (for the remaining part of the region not covered by triangular prism elements) (Figure

2). The selection of the number degrees of freedom (NDOF) values follows the requirements that the boundary conditions given by the stresses should be satisfied with very high accuracy and the numerical results obtained for the various NDOFs should converge.

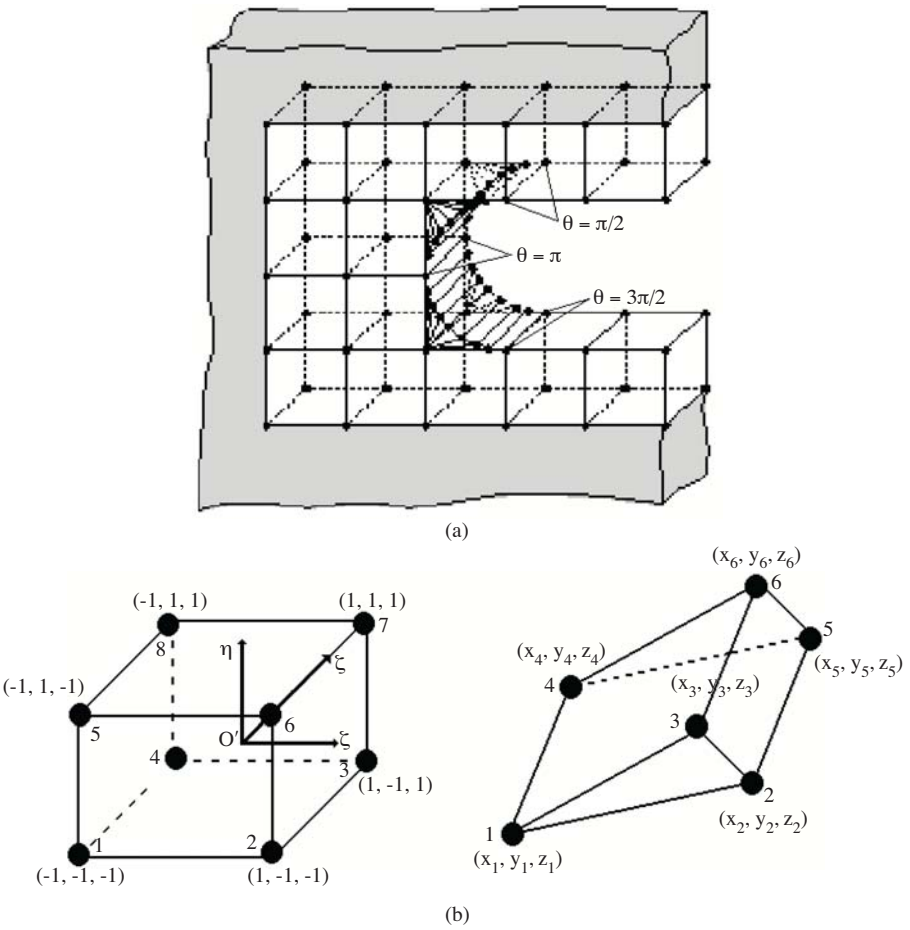

Figure 2. a) The finite elements mesh around the cylindrical hole; b) The geometry of the brick and the triangular prism finite elements.

Solution method requires that the region $(\Omega - \Omega')$ occupied by the plate be presented as the combination of the finite elements given below:

$$(\Omega - \Omega') = \bigcup_{k=1}^{M} \Omega_k \tag{9}$$

where Ω_k is the k^{th} finite element.

Within each finite element Ω_k displacements are expressed with the shape functions and unknown displacements at nodes;

$$\mathbf{u^{(k)}} \approx \mathbf{N^{(k)}}\mathbf{a^{(k)}}, K = 1, 2, \ldots, M \tag{10}$$

where

$$\left(\mathbf{a^{(k)}}\right)^T = \left\{u_{11}^k, u_{21}^k, u_{31}^k, u_{12}^k, u_{22}^k, u_{32}^k \ldots, u_{1p}^k, u_{2p}^k, u_{3p}^k\right\} \quad ,$$

$$\left(N^{(k)}\right)^T = \left\{ \begin{array}{cccccccccc} N_1^k & 0 & 0 & N_2^k & 0 & 0 & ... & N_p^k & 0 & 0 \\ 0 & N_1^k & 0 & 0 & N_2^k & 0 & ... & 0 & N_p^k & 0 \\ 0 & 0 & N_1^k & 0 & 0 & N_2^k & ... & 0 & 0 & N_p^k \end{array} \right\},$$

$$\left(u^{(\mathbf{k})}\right)^T = \left\{u_1^k\left(x_1,x_2,x_3\right), u_2^k\left(x_1,x_2,x_3\right), u_3^k\left(x_1,x_2,x_3\right)\right\}. \tag{11}$$

In Eq. (11) p equals 8 (6) for a brick (a triangular prism) finite element. Substituting Eq. (10) into Eq. (6) and Eq. (7), after some mathematical manipulations, finally yields the following system of algebraic equations:

for the first boundary-value problem (2),

$$\mathbf{K}^{(0)}\mathbf{a}^{(0)} = \mathbf{r}^{(0)} \tag{12}$$

and for the second boundary-value problem ((3)-(5))

$$K\,\mathbf{a} = \mathbf{r} \quad . \tag{13}$$

In Eqs. (12) and (13) $\mathbf{K}^{(0)}$ and $\mathbf{K}$ are the stiffness matrixes, $\mathbf{a}$ is the vector the components of which are the displacements at the nodes, and $\mathbf{r}^{(0)}$ and $\mathbf{r}$ are the force vectors [12].

The solutions to Eqs. (12) and (13) give the values of the displacements at the nodes. However, the equation (13) includes the values of the stresses from the first boundary-value problem. Therefore, before finding the solution to Eq. (13), the distributions of stresses for the first problem should be found. Using the solution to Eq. (12) and Hooke's law (given in Eq. (2)), these can be obtained.

Note that the numerical solution to both considered problems are modeled with the same finite elements and the same arrangements.

Numerical Results and Discussion

Assume that the material of the plate is a composite consisting of a large number of alternating layers of 2 materials. Suppose that the material of each layer is isotropic and these layers are located on the planes $x_2 = const$. The values related to the matrix and to the reinforcing material is indicated by the subscripts 1 and 2, respectively. Let λ_k and μ_k be the Lamé constants; E_k, the Young module; ν_k, the Poisson's ratios, and η_k, the concentrations of the components in the representative pack. Assume that the plate material is transversally isotropic with the symmetry axis Ox_2, and the effective mechanical constants A_{ij} (in (2)) are given below (Akbarov and Guz, 2000)

$$A_{23} = A_{12} = \lambda_1\eta_1 + \lambda_2\eta_2 - \eta_1\eta_2\left(\lambda_1 - \lambda_2\frac{(\lambda_1+2\mu_1)-(\lambda_2+2\mu_2)}{(\lambda_1+2\mu_1)\,\eta_2+(\lambda_2+2\mu_2)\,\eta_1}\right),$$

$$\frac{1}{2}\left(A_{11}+A_{12}\right) = (\lambda_1+2\mu_1)\,\eta_1 + (\lambda_2+2\mu_2)\,\eta_2 - \frac{(\lambda_1-\lambda_2)^2}{(\lambda_1+2\mu_1)\,\eta_2+(\lambda_2+2\mu_2)\,\eta_1},$$

$$\frac{1}{2}\left(A_{11}-A_{13}\right) = \eta_1\mu_1 + \eta_2\mu_2,$$

$$A_{66} = A_{44} = \frac{\mu_1\mu_2}{\mu_1\eta_2+\mu_2\eta_1}, A_{55} = \eta_1\mu_1 + \eta_2\mu_2, \quad A_{11} = A_{33},$$

$$A_{22} = (\lambda_1 + 2\mu_1)\,\eta_1 + (\lambda_2 + 2\mu_2)\,\eta_2 - \eta_1\eta_2 \frac{((\lambda_1 + 2\mu_1) - (\lambda_1 + 2\mu_2))^2}{(\lambda_1 + 2\mu_1)\,\eta_2 + (\lambda_2 + 2\mu_2)\,\eta_1}. \tag{14}$$

Consider the case where the geometry of plate has symmetry with respect to $x_1 = \ell_1/2$ and $x_3 = \ell_3/2$ planes. So FEM solutions are obtained in a quarter part of the domain. This domain is divided into 30, 40, and 12 brick elements in the direction of Ox_1, Ox_3 and Ox_2 axes, respectively but 16 triangular prism elements surround the cylindrical hole in a layer. For the FEM modeling, 13,440 brick elements and 640 triangular prism finite elements, 16,605 nodes and 49,282 NDOFs have been used in total.

Note that before obtaining the numerical results, the PC programs composed by the author are tested on the problems considered in the papers (Akbarov et al., 2004; Akbarov et al., 2008; Yahnioglu and Babuscu Yesil, 2009).

In the present paper, due to understandable difficulties in dealing with the clarity of the graphs, all graphics are illustrated in the cylindrical coordinate system and given at the plane $x_3 = \ell_3/2$. The values of all the parameters are given in the figures.

Figure 3 shows the influence of the initial stretching, i.e. q/E_1, on the values of $\sigma_{\theta\theta}/p$ at the mid-point of each element around the cylindrical hole on the $x_3 = \ell_3/2$ plane for $E_2/E_1 = 1$ (i.e. for an isotropic thick plate) and $E_2/E_1 = 10$ (i.e. for an anisotropic thick plate). As can be seen in the figures, it is concluded that the absolute value of $\sigma_{\theta\theta}/p$ significantly decreases with initial stretching force and the more the initial stretching force is applied, the more the difference is between the $\sigma_{\theta\theta}/p$ obtained for $q/E_1 = 0$ and the $\sigma_{\theta\theta}/p$ obtained for $q/E_1 \neq 0$.

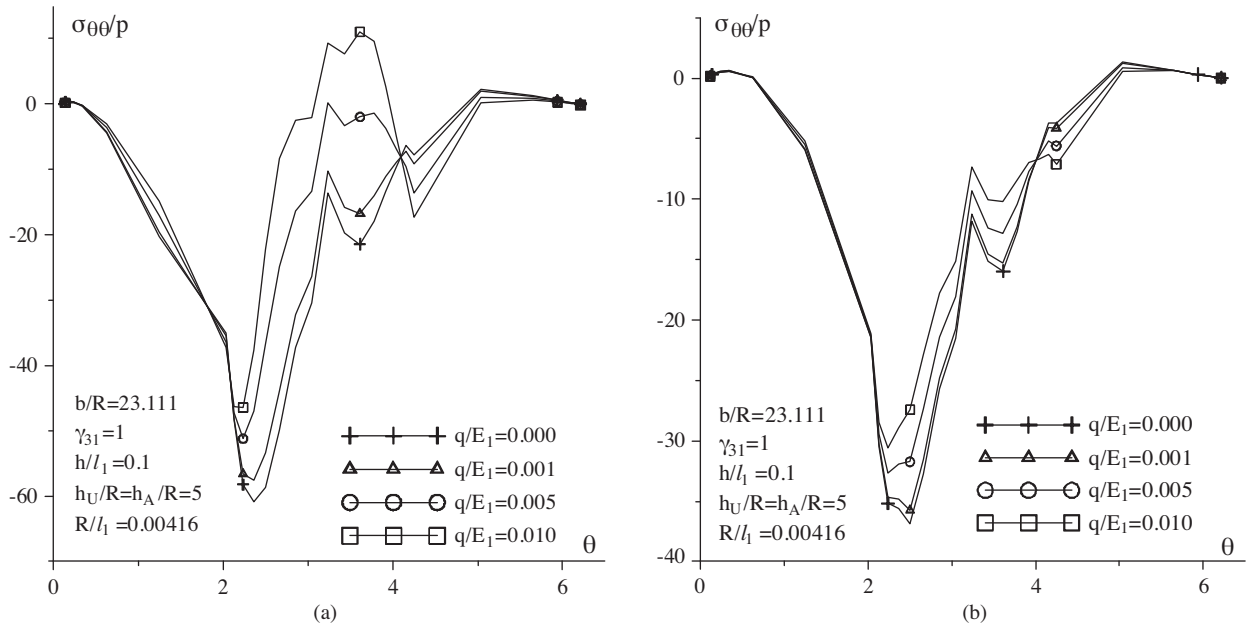

Figure 3. The influence of q/E_1 on the values of $\sigma_{\theta\theta}/p$. a) For $E_2/E_1 = 1$, b) For $E_2/E_1 = 0$.

Figure 4 shows the distribution of $\sigma_{\theta\theta}/p$ on the surface of the cylindrical hole for a quarter region of the plate. It follows from the graphs that the absolute maximum values of $\sigma_{\theta\theta}/p$ occur around the $x_3/\ell_3 = 1/2$ plane.

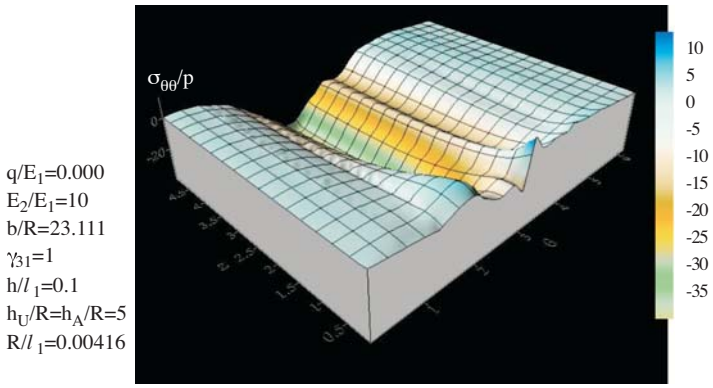

Figure 4. The distribution of the stress $\sigma_{\theta\theta}/p$ on the surface of the cylindrical hole.

Figures 5 and 7 show the influence of the initial stretching, i.e. q/E_1, on the values of u_r and u_θ at the mid-point of each element around the hole for $E_2/E_1 = 1$ and $E_2/E_1 = 10$. It follows from the graphs that the absolute maximum values of all the displacements decrease with q/E_1. The values of the displacement u_z are smaller than those of the other displacements.

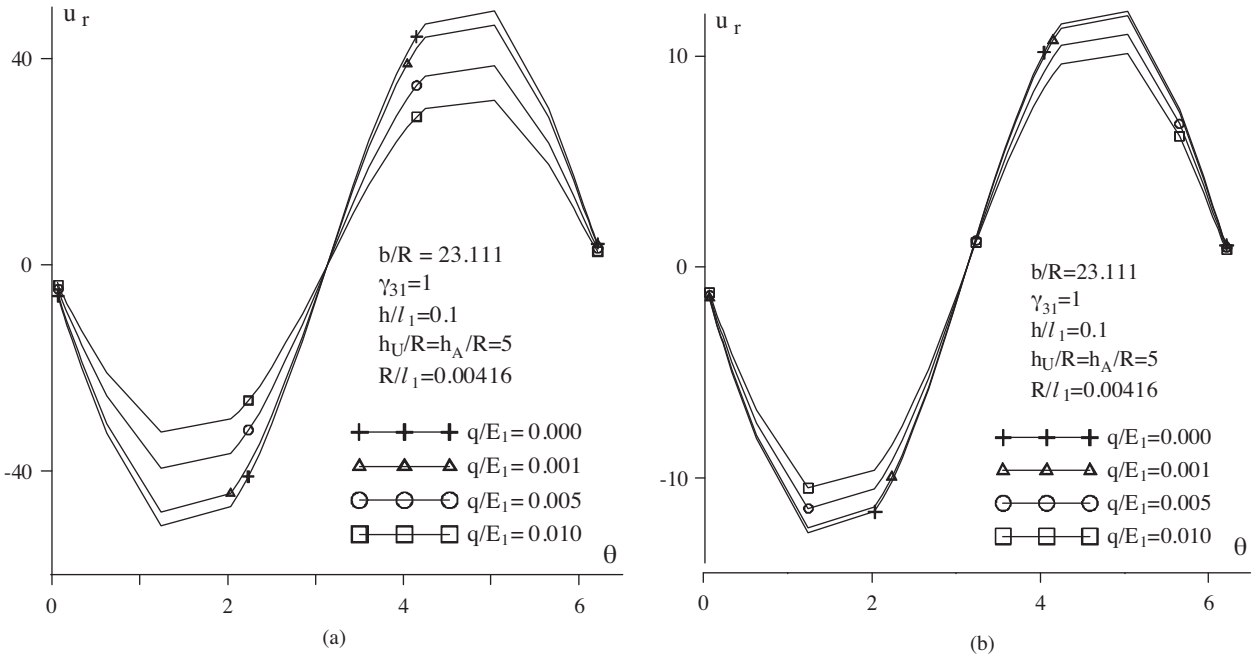

Figure 5. The influence of q/E_1 on the values of u_r; a) For $E_2/E_1 = 1$, b) For $E_2/E_1 = 10$.

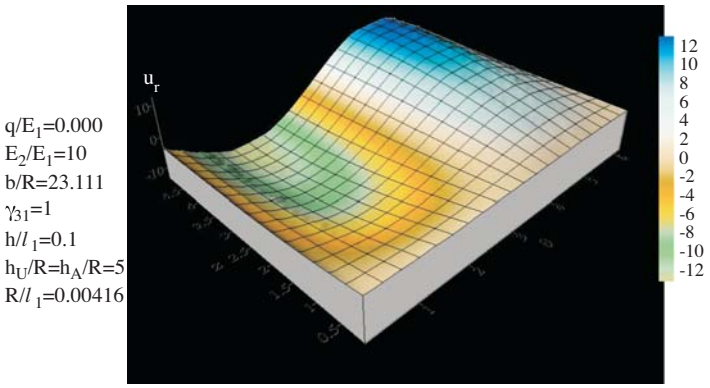

Figure 6. The distribution of the displacement u_r on the surface of the cylindrical hole.

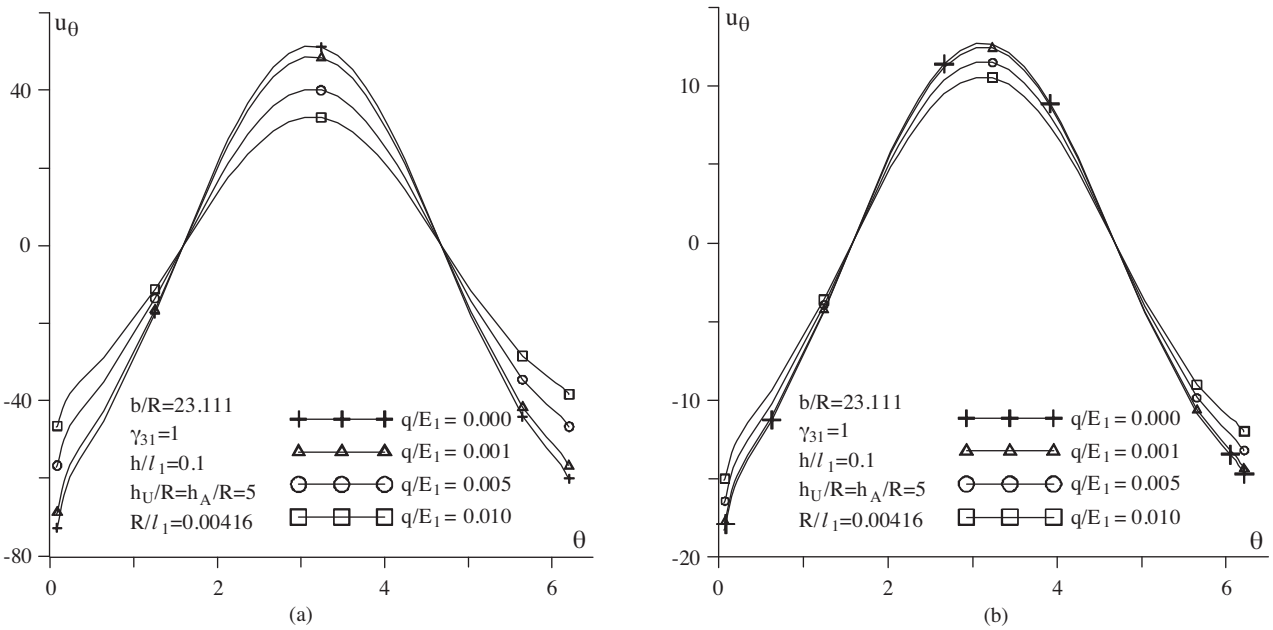

Figure 7. The influence of q/E_1 on the values of u_θ; a) For $E_2/E_1 = 1$, b) For $E_2/E_1 = 10$.

The distributions of u_r, u_θ, and u_z on the surface of the cylindrical hole are given in Figures 6, 8, and 9.

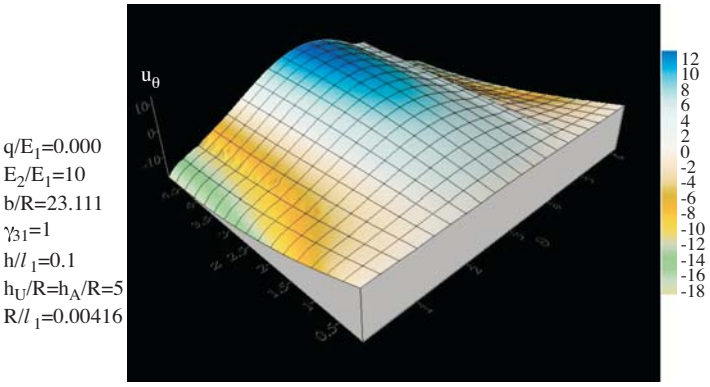

Figure 8. The distribution of the displacement u_θ on the surface of the cylindrical hole.

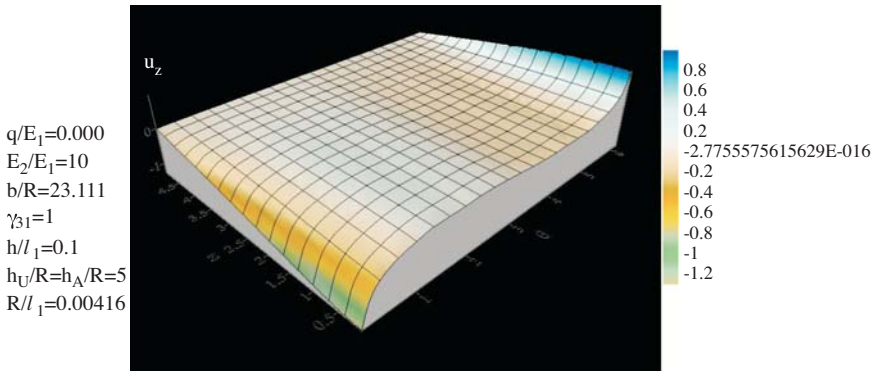

Figure 9. The distribution of the displacement u_z on the surface of the cylindrical hole.

Figure 10 shows the influence of the ratio b/R(where b (R) is the half length of the hole along the $Ox_1(Ox_2)$ axis) on the values of $\sigma_{\theta\theta}/p$. In this case the increase of the b/R causes the increase of the volume of the hole. It follows from the graphs that the absolute values of $\sigma_{\theta\theta}/p$ increase monotonically with b/R and decrease with the initial stretching q/E_1.

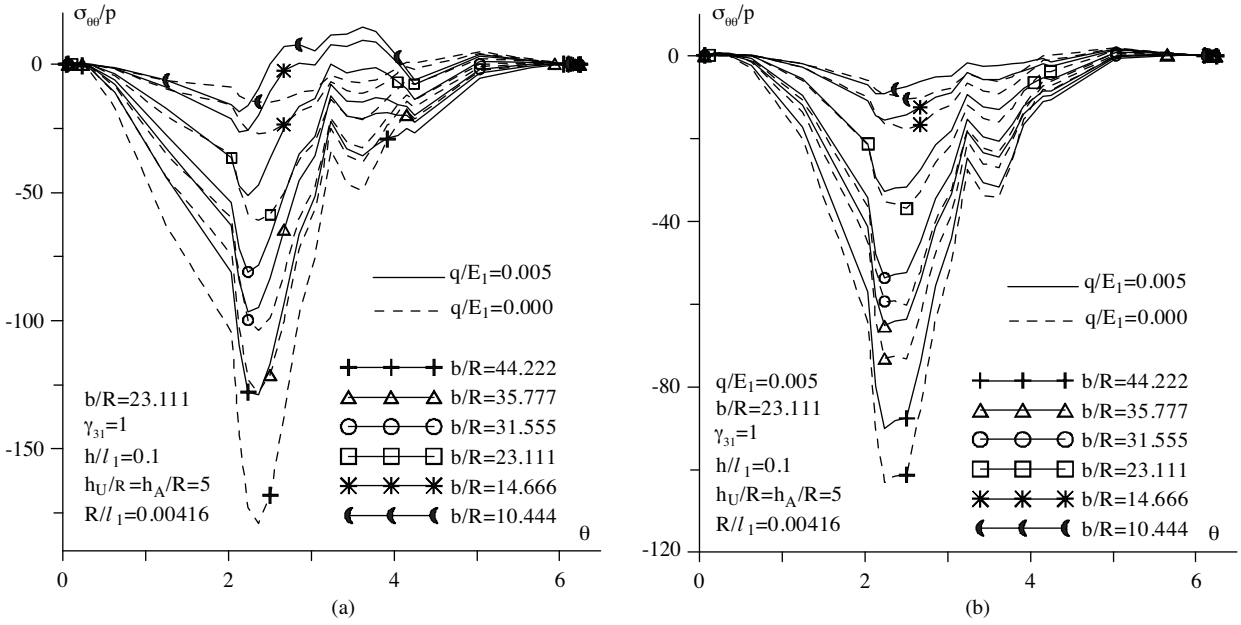

Figure 10. The influence of b/R on the values of $\sigma_{\theta\theta}/p$ for a)$E_2/E_1 = 1$, b) $E_2/E_1 = 10$.

Figures 11-13 show the influence of the anisotropy (i.e. the values of E_2/E_1) on the values of $\sigma_{\theta\theta}/p$,u_r and u_θ, respectively. It follows from these graphs that the absolute maximum values of $\sigma_{\theta\theta}/p$,u_r, and u_θ decrease with E_2/E_1. Following from these graphs, it is concluded that the difference between the values of $\sigma_{\theta\theta}/p$, u_r, and u_θ for $q/E_1 = 0$ and the values of $\sigma_{\theta\theta}/p$, u_r and u_θ for $q/E_1 \neq 0$ increase with E_2/E_1.

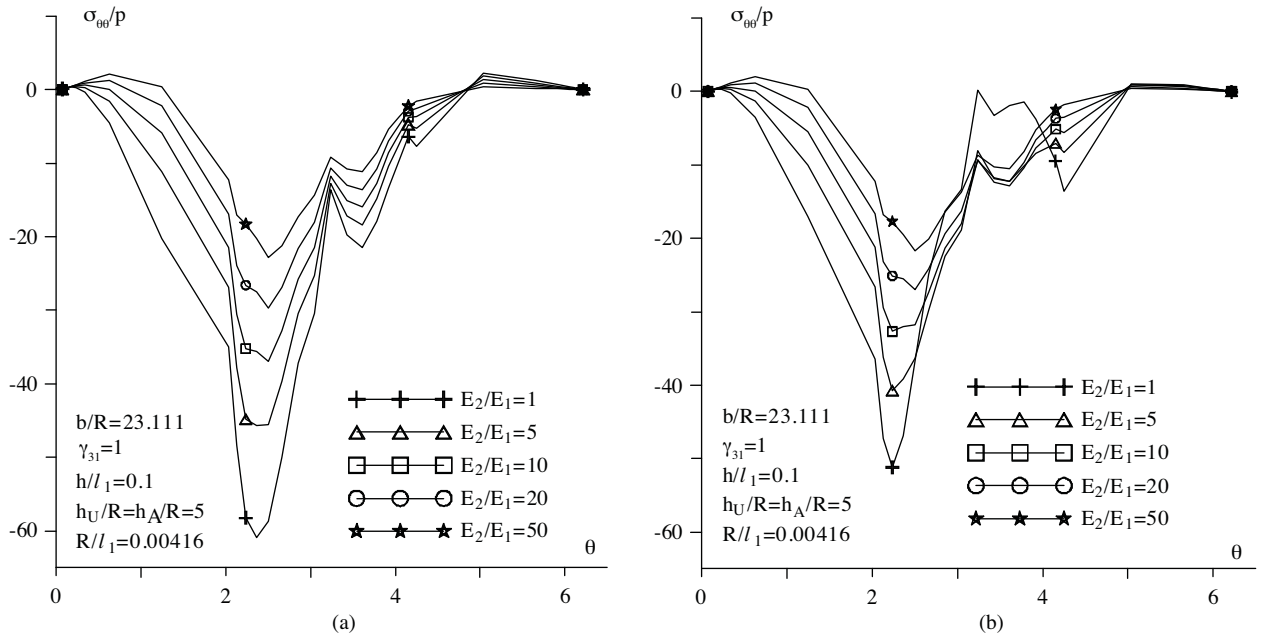

Figure 11. The influence of E_2/E_1 on the values of $\sigma_{\theta\theta}/p$ for a) $q/E_1 = 0$, b) q/E_1 =0.005.

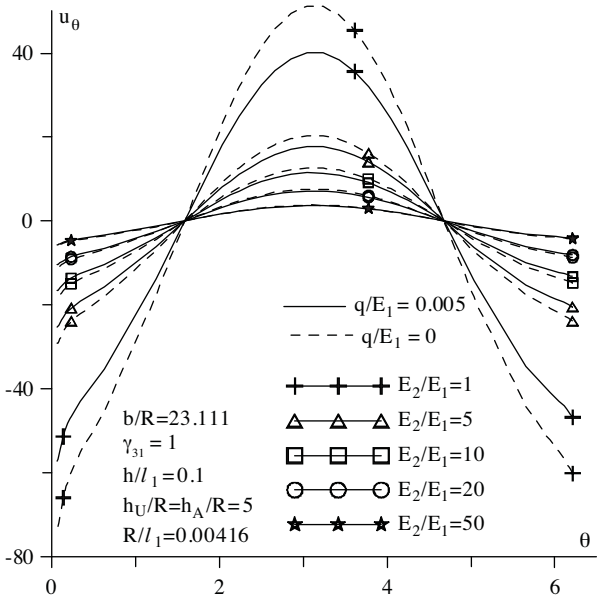

Figure 12. The influence of E_2/E_1 on the values of u_r.

Figures 14 shows the influence of the hole's location on $\sigma_{\theta\theta}/p$. The parameter h_U/R shows the thickness of the part of the plate at the top of the hole. Therefore, while the value of h_U/R decreases, the hole changes its location entirely and moves closer to the upper face plane of the plate. It follows from the graphs that the absolute values of $\sigma_{\theta\theta}/p$ increase monotonically with the decreasing h_U/R for the cases where $q/E_1 \neq 0$ and$q/E_1 = 0$.

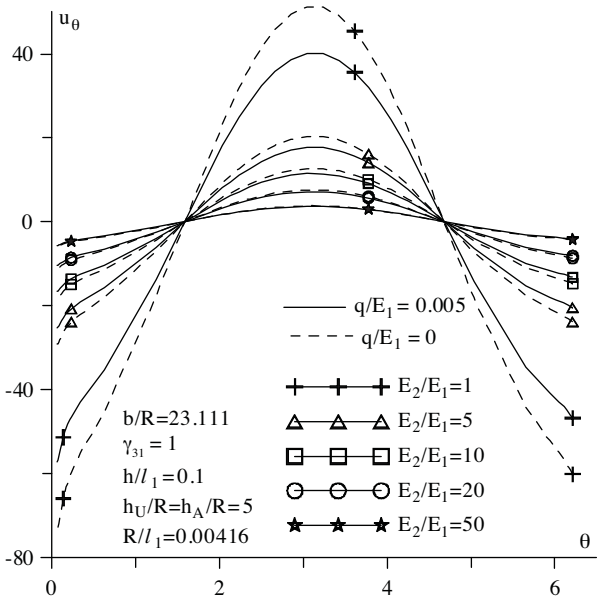

Figure 13. The influence of E_2/E_1 on the values of the displacement u_θ.

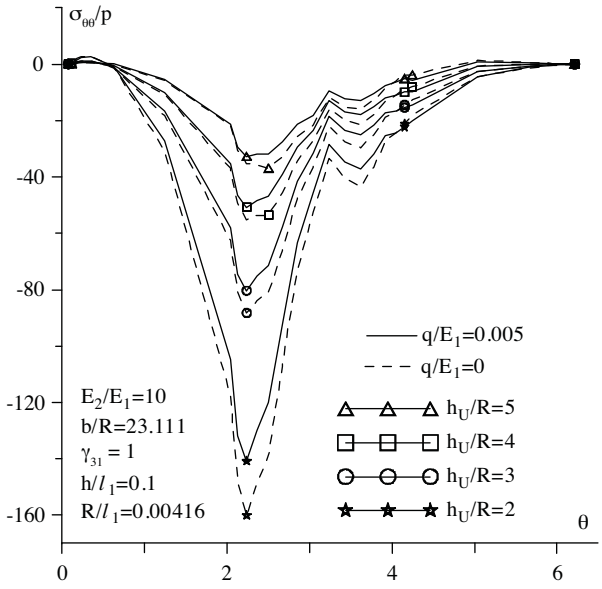

Figure 14. The influence of h_u/R on the values of $\sigma_{\theta\theta}/p$ for $q/E_1 = 0$ and $q/E_1 = 0.005$.

Figures 15 and 16 show the influence of $\gamma_{31} = \ell_3/\ell_1$ on the values of $\sigma_{\theta\theta}/p$ for the case where $E_2/E_1 = 1$ (for $q/E_1 = 0.0$ and $q/E_1 = 0.005$) and $E_2/E_1 = 10$ (for $q/E_1 = 0.0$ and $q/E_1 = 0.005$). $\gamma_{31} = \ell_3/\ell_1$ shows the ratio of the 2 lengths along the 2 perpendicular directions, i.e. the length of the thick plate along the Ox_3 axis (denoted by ℓ_3) and along the Ox_1 axis (denoted by ℓ_1). It follows from the graphs that the absolute values of $\sigma_{\theta\theta}/p$ increase monotonically with increasing $\gamma_{31} = \ell_3/\ell_1$ for the cases where $q/E_1 \neq 0$, $q/E_1 = 0$, and $E_2/E_1 = 1$, $E_2/E_1 = 10$, and approach the limit values, i.e. the values determined from the corresponding boundary-value problem in the plane-strain state. These results confirm the trustiness of the algorithm and the PC programs composed by the author and used for the determination of the numerical solution.

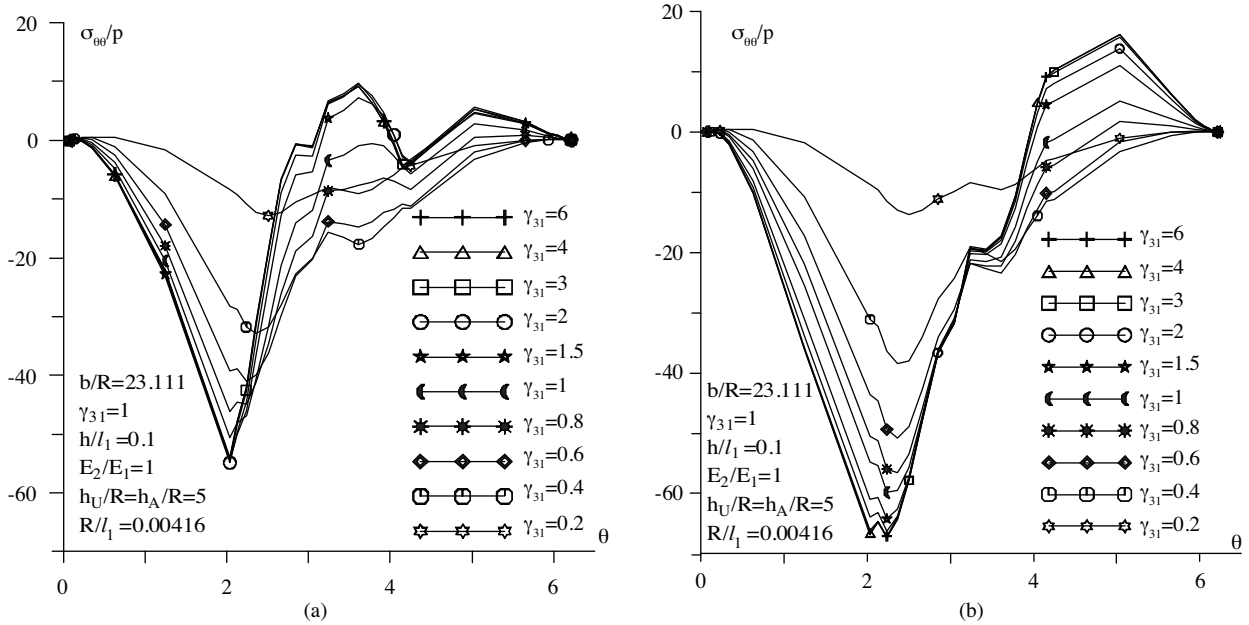

Figure 15. The influence of $\gamma_{31} = \ell_3/\ell_1$ on the values of $\sigma_{\theta\theta}/p$ for $E_2/E_1 = 1$ and for a) $q/E_1 = 0$, b) q/E_1 =0.005.

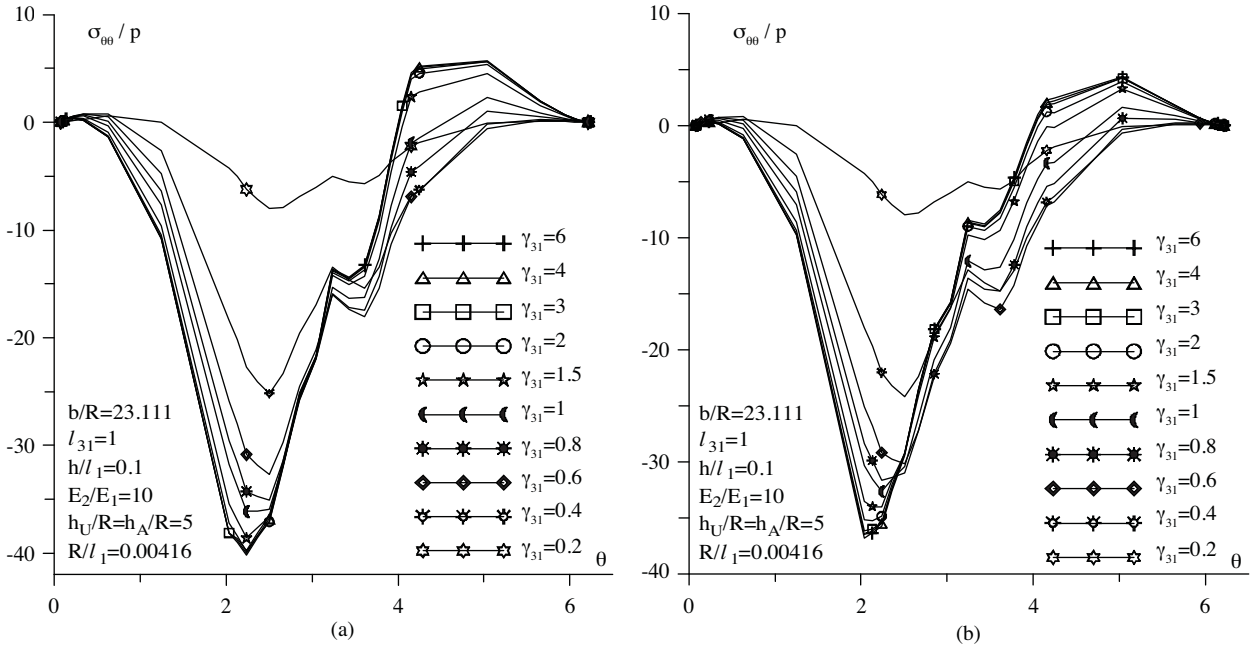

Figure 16. The influence of γ_{31} on the values of $\sigma_{\theta\theta}/p$ for $E_2/E_1 = 10$ and for a) $q/E_1 = 0$, b) q/E_1 =0.005.

Conclusion

In the present paper, stress and displacement distributions of an initially statically stressed plate containing an internal cylindrical hole (lying width-wise in the plate) given a rectangular cross section with rounded off corners is studied. The investigation focuses on the effect of the initial stresses on the stress and displacement distributions arising as a result of the action of the additional static forces. The governing equation is derived

within the scope of the 3-dimensional linearized theory of elasticity in initially stressed bodies. The 3D finite elements method is employed so as to provide a solution to the corresponding boundary-value problems. The numerical results on the stress and displacement concentrations around the hole and the influence of the initial stresses and other problem parameters on these stresses are presented and discussed. Based on these analyses, the following concrete conclusions can be drawn:

- The absolute value of $\sigma_{\theta\theta}/p$ significantly decreases with the initial stretching force and the more the initial stretching force is applied the more the difference is between the $\sigma_{\theta\theta}/p$ obtained for $q/E_1 \neq 0$.
- The absolute maximum values of all the displacements decrease with q/E_1. The values of the displacement u_z are smaller than those of the other displacements.
- The absolute values of $\sigma_{\theta\theta}/p$ increase monotonically with b/R and decrease with the initial stretching $q/E_2/E_1$.
- The absolute maximum values of $\sigma_{\theta\theta}/p$,u_r, and u_θ decrease with E_2/E_1. The difference between the values of $\sigma_{\theta\theta}/p$, u_r, and u_θ for $q/E_1 = 0$ and the values of $\sigma_{\theta\theta}/p$, u_r, and u_θ for $q/E_1 \neq 0$ increase with E_2/E_1.
- The absolute values of $\sigma_{\theta\theta}/p$ increase monotonically with the decreasing h_U/R for the cases where $q/E_1 \neq 0$ and $q/E_1 = 0$.
- The absolute values of $\sigma_{\theta\theta}/p$ increase monotonically with increasing $\gamma_{31} = \ell_3/\ell_1$ for the cases where $q/E_1 \neq 0$, $q/E_1 = 0$ and $E_2/E_1 = 1$, $E_2/E_1 = 10$, and approach the limit values, i.e. the values determined from the corresponding boundary-value problem in the plane-strain state.

Nomenclature

Ω	domain of full plate
Ω'	domain of cylindrical hole
$(\Omega - \Omega')$	solution domain
$Ox_1x_2x_3$	Cartesian coordinate system
(x_{01}, y_{01})	center of the left half circular arc in the plane $x_3 = \text{const.}$
(x_{02}, y_{02})	center of the right half circular arc in the plane $x_3 = \text{const.}$
h_A	height of the part of the plate at the bottom of the hole
h_U	height of the part of the plate at the top of the hole
p	additional uniformly distributed normal forces
q	initial state the uniformly distributed normal stretching forces
ℓ_1	length of the thick plate along the axis Ox_1
ℓ_3	length of the thick plate along the axis Ox_3
A_{ij}	effective material constants
σ_{ij}	components of stresses
$\sigma_{ij}^{(0)}$	initial stresses in the considered plate
δ_i^j	kronecker symbol
S	surface of the cylidrical hole
n_j	components of the unit normal vector
NDOF	number degrees of freedom
$K^{(0)}, K$	stiffness matrixes

a	the vector the components of which are the displacements at the nodes
$r^{(0)}, r$	force vectors
λ_k and μ_k	Lamé constants
E_k	young Module
ν_k	Poisson's ratios
η_k	concentrations of the components in composite materials
b	half length of the hole along the Ox_1 axis
R	half length of the hole along the Ox_2 axis
u_r	displacement through the axis $O'r$in the cylindrical coordinates $O'r\theta z$
u_θ	displacement through the axis $O'\theta$ in the cylindrical coordinates $O'r\theta z$
u_z	displacement through the axis $O'z$ in the cylindrical coordinates $O'r\theta z$

Acknowledgments

The author is grateful to Prof. Dr. Surkay D. AKBAROV and Prof. Dr. Nazmiye YAHNİOĞLU for comments and discussion and to the Scientific and Technological Research Council of Turkey (TÜBİTAK) for the financial support.

References

Akbarov, S.D. and Guz, A.N., Mechanics of Curved Composites, Dordrecht, The Netherlands, Kluwer, 441, 2000.

Akbarov, S. D., Yahnioglu, N. and Yucel A. M., "On the Influence of the Initial Tension of a Strip with a Rectangular Hole on the Stress Concentration Caused by Additional Loading", The Journal of Strain Analysis for Engineering Design, **39**(4), 615 – 624, 2004**.**

Akbarov, S.D., Yahnioglu, N. and Yesil, U., "Interaction Between Two Neighbouring Circular Holes in a Pre-Stretched Simply Supported Orthotropic Strip Under Bending", Mechanics of Composite Materials, 44 (4), 827-838, 2008.

Chaudhuri, R. A., "Weakening Effects of Internal Part-Through Elliptic Holes in Homogeneous and Laminated Composite Plates", Composites Structures, 81, 362-373, 2007.

Guz, A.N., Fundamentals of the Three-Dimensional Theory of Stability of Deformable Bodies, Springer-Verlag- Berlin, 1999.

Jain N.K. and Mittal N.D., "Finite Element Analysis for Stress Concentration and Deflection in Isotropic, Orthotropic and Laminated Composite Plates With Central Circular Hole Under Transverse Static Loading", Materials Science and Engineering A, 498, 115-124, 2008.

Lei, G.H., Charles, W.W. Ng. and Rigby, D.B., "Stress and Displacement Around an Elastic Artificial Rectangular Hole", Journal of Engineering Mechanics, 127(7) 880-890, 2001.

Savin, G.N., Stress Concentration Around Holes, E. Gros Translator, Pergomon, 1961.

Temiz, S., Özel, A. and Aydın, M.D., "Fem Stress Analysis of Thick Composite Laminates With a Hole in Bending", Applied Composite Materials, 10, 103–117, 2003.

Toubal, L.T., Karama, M. and Lorrai B., "Stress Concentration in a Circular Hole in Composite Plate", Composite Structures, 68 (1), 31-36, 2005.

Yahnioglu N. and Babuscu Yesil U., "Forced Vibration of an Initial Stressed Rectangular Composite Thick Plate With a Cylindrical Hole", ASME 2009 International Mechanical Engineering Congress and Exposition IMECE09 November 13-19, 2009, Lake Buena Vista, Florida, USA. 2009.

Zheng Y., Chang-Boo K., Chongdu C. and Hyeon Gyu B., "The Concentration of Stress and Strain in Finite Thickness Elastic Plate Containing a Circular Hole", International Journal of Solids and Structures, 45(3-4), 713-731, 2008.